Journal of Advances in Science, Engineering and Technology

Hybrid Precoding for Multi-Cell mmWave Multiuser Massive MIMO 5G Networks

Enos Simiyu, Filbert Ombongi*, Raymond Juma

[a]*Department of Electrical and Communications Engineering, School of Engineering and Built Environment, Masinde Muliro University of Science and Technology, Kakamega, Kenya.*

ABSTRACT

In recent times, there has been a rapid growth in the data traffic demand. The 5G millimeter wave technology has been deployed to offer a large bandwidth resource for cellular systems. However, the millimeter wave communication suffers from high path losses. Therefore, there is a need to implement a high number of antennas to overcome the high propagation losses and offer beam-forming gain. Multiple-Input Multiple-Output is a wireless technology that uses multiple antennas at both the transmitter and receiver to enhance performance by increasing reliability and data speeds. The Multiple-Input Multiple-Output technology has the potential of meeting the need for high network capacity in the next generation cellular networks since it can offer improved power and spectrum efficiency. When massive Multiple-Input Multiple-Output is deployed in a multi-cell environment, inter-cell interference goes up as the cell edge users are approached. It also results in pilot contamination due to the frequent reuse of the pilots in each cell. In this paper, a Single Value Decomposition-based hybrid precoding scheme was formulated as a spectral efficiency maximization problem for multi-cell multi-user millimeter wave massive Multiple-Input Multiple-Output by minimizing channel estimation errors and inter-cell interference. The model was simulated in MATLAB, and the results for the full and partial connection scenarios. The results showed a 1.6381 times improvement in performance in terms of spectrum efficiency and normalized minimum square error when compared to the compressive sensing algorithm.

ARTICLE INFO

Keywords:
mmWave,
Massive MIMO,
multi-cell,
Inter-cell interference.

Article History:
Received 20 May 2025
Received in revised form 21 October 2025
Accepted 7 November 2025
Available online 10 December 2025

1. Introduction

The future demand for channel capacity and spectral efficiency in 5G and subsequent wireless communication is expected to be high. The millimeter wave (mmWave) Multiple-Input Multiple-Output (MIMO) technology has been deployed to meet this demand (Sha, Wang, Chen, & Hanzo, 2020). The mmWave has higher bandwidth resources and, as such, the mmWave communication has attracted much attention from the research community to meet the requirements of the future networks (Heath, Gonzalez-Prelcic, Ranguan, Roh, & Sayeed, 2016). However, mmWave signals experience high propagation path loss due to their high frequency. The high propagation path loss challenge can be overcome by deploying a massive MIMO antenna array to realize directional beam alignment and data transmission. The large antenna arrays can be packed into small form factors due to the shorter wavelength mmWave bands. This implies that the channel estimation requires a large time slot overhead. It should also be noted that mmWave channels have a sparsity feature in the beam space domain, where the beam space channels can be formed by either the lens antenna arrays or phase shifter network (Gao, Hu, Dai, & Wang, 2016; Rodriguez-Fernandez, Gonzalez-Prelcic, Venugopal, & Heath, 2018). The large number of antennas in mmWave MIMO makes the dimensionality of the channel matrix very high, which leads to complex and challenging channel estimation. The accurate Channel State Information (CSI) can be obtained by transmitting pilot sequences from multiple antenna pairs. However, the transmission of pilots from multiple antenna pairs leads to mutual interference between pilots, which in turn requires additional channel resources and feedback delay.

However, a conventional MIMO multi-user environment is prone to inter-cell interference (ICI) that arises mainly due to pilot contamination from adjacent

* Corresponding author. e-mail: enos.sim@gmail.com
Editor: Gershom Mutua, Masinde Muliro University of Science and Technology, Kenya.
Citation: Simiyu E., Ombongi F., & Juma R. (2025). Hybrid Precoding for Multi-Cell mmWave Multiuser Massive MIMO 5G Networks. Journal of Advances in Science, Engineering and Technology 2(1), 78 – 86.

© 2025 Creative Commons Attribution License (CC BY-NC-SA).

cells. This can be overcome by implementing a combination of mmWave MIMO systems with channel estimation techniques and 3D beam-forming techniques to suppress ICI. In mobile communication systems, ICI is among the major challenges that degrade system performance, especially for cell-edge users and in densely populated cells (Ally, 2023).

Some studies have proposed channel estimation architectures that are either purely analog, purely digital, or hybrid to increase channel capacity. The hybrid channel estimation architectures can be based on tensor theory (Hao, Luo, Li, & Fan, 2024; Hong, Sun, He, Zhang, & Wang, 2024), beam squint (Wang, Jian, Gao, Li, & Lin, 2019; Xu, Cheng, Wong, Wu, & Poor, 2024) compressive sensing (Oyerinde, Flizikowski, & Marciniak, 2022; Gao, Mei, & Qiao, 2022), random spatial sampling based beam forming (Vlachos, Alexandropoulos, & Thompson, 2019; Vadgaye & Manjula, 2024), and time domain (Kim, Gil, & Lee, 2019). However, these channel estimation algorithms don't give full diversity (tensor-based), low convergence for a large number of antennas (compressive sensing), difficulty of getting the initial parameters (random spatial sampling), and diversity gain not being enhanced further for time domain-based hybrid precoding.

Therefore, the current study considers channel estimation algorithms based on a combination of algorithms to overcome convergence and diversity gain in mmWave massive MIMO systems in the context of a multi-cell network scenario. The massive MIMO channel estimation techniques are categorized into three, i.e., pilot-based, blind, and semi-blind channel estimation. The pilot-based technique rebuilds the channel response by employing a priori channel information, leading to better accuracy and reliability. The commonly used pilot-based channel estimation algorithms include least square (LS) estimation (Riadi, Boulouird, & Hassani, 2019) and minimum mean square error (MMSE) estimation (Li, Song, Ahmad, & Swamy, 2014). The LS channel estimation algorithm is characterized by its lower computational complexity. However, it does not account for the influence of noise. It relies on the error between the actual observations and the estimated observations, which makes it particularly susceptible to noise enhancement in practical applications. This susceptibility is especially pronounced when the channel experiences large-scale fading, leading to significant degradation in the accuracy of channel estimation. This challenge can be overcome by developing an MMSE-based channel estimation algorithm that directly uses the error between the true value of the estimator and the estimated value as the optimization objective. This eventually brings down the effect of noise, producing a more accurate channel estimation.

Hence, with an increase in the number of antennas in massive MIMO communication systems, the complexity of the algorithm increases, presenting challenges for its effective implementation in practical engineering applications. A modified MMSE, named as linear minimum mean square error (LMMSE) channel estimation algorithm, can be used to overcome this challenge. It incorporates a linear smoothing process based on MMSE channel estimation and eliminates one matrix inverse operation, and utilizes expected values instead of true values. This modified algorithm sacrifices performance in exchange for lower computational complexity.

Some of the issues that have not been handled under pilot contamination are its effect on the data rate achievable and its contribution to the network or systems performance in the mmWave massive MIMO network. The application of channel estimation and pilot assignment jointly in a hybrid mmWave multi-cell network is another challenge that has been handled in this study. In ICI, the user density and the massive number of antenna elements are some of the challenges that have not been dealt with to improve the network performance in the mmWave massive MIMO.

The Single Value Decomposition (SVD)-based hybrid precoding, which is a key contribution in the current study, offers some merits compared to alternating minimization and compressive sensing schemes, which have been applied in massive MIMO. To start with, the SVD avoids the iterative optimization in determining the analog precoding matrices. When it is combined with hybrid precoding, there is low power consumed in the network, thereby improving the energy efficiency. In addition, the SVD-based hybrid precoding can optimally result in a low convergence rate, and it provides a foundation for developing effective and efficient networks. The compressive sensing and alternating minimization are characterized by additional complexity if the number of cells, users, and antenna elements goes up, which requires significant computing resources to attain a low rate of convergence. In Oyerinde, Flizikowski, & Marciniak (2022) and Gao, Hu, Dai, & Wang (2016), the methods used have not taken into consideration the effect of multi-cell, dense users and a large number of antenna elements in the mmWave Massive MIMO network. In addition, the number of users under consideration is low (2 and 4 user scenarios) in a single cell. However, in the current study, the effect of dense users and, large number of antenna elements on the network performance is considered.

The key contributions of this study include: To develop an SVD-based hybrid precoding in a multi-cell mmWave massive MIMO in a multiuser scenario by utilizing hybrid architectures and algorithms to maximize spectrum efficiency for full and partial connections. To study the effect of increasing the number of antenna elements at the transmitter on spectrum efficiency for a multi-cell massive MIMO network. To determine the effect of user density on the MMSE for different signal-to-interference-noise ratios (SINRs).

2. Materials and Methods

2.1. System Model

The main goal of this study is to mitigate ICI in multi-cell mm-wave MIMO systems characterized by a multiuser scenario. It incorporates hybrid precoding/

beamforming and channel estimation techniques to maximize the sum rate. The first step deals with ICI in the channel estimation process, the beam space idea is fully utilized to select beams of all the mobile units and carefully select the in-cell mobile units' beams as per the position information available (CSI). Then, the estimation of spatial frequencies within the beam space follows. Selected beams are matched with these estimates. The in-cell mobile unit beams, as well as the mobile units in other cells, are selected. The mobile units with the same pilots are placed away from each other to ensure effective ICI mitigation. Table 1 shows the main parameters used for simulation.

Table 1: Simulation Parameters

Parameter	Symbol	Value
Number of Cells	L	7
Signal-to-noise ratio	γ	-30-30
Number of RF chains at transmitter	N_T^{RF}	16
Number of RF chains in each user	N_R^{RF}	4
Number of transmit antennas	$M\ or\ N_T$	16-128
Number of receiver antennas	N_R	4-128
Number of paths	N_P	3
Carrier frequency	f_c	28GHz
Number of Users	K	4-100

2.2. System modelling for a Multicell mmWave Massive MIMO

Consider a multicell mmWave massive MIMO having L cells and each cell has a Base Station (BS) at the centre with M antennas serving a set of K single antenna users referred as User Equipment (UEs) as shown in Fig. 1. It should be noted that in a massive MIMO network the number of antennas is greater than number of users ($M \gg K$). The L cells share the same mmWave band of frequencies.

The average transmission power at the base station is p_t and the received power at each mobile user is p_r. The system uses the OFDM working in time division duplex (TDD). The channel gain matrix is determined by large and small-scale fading coefficients.

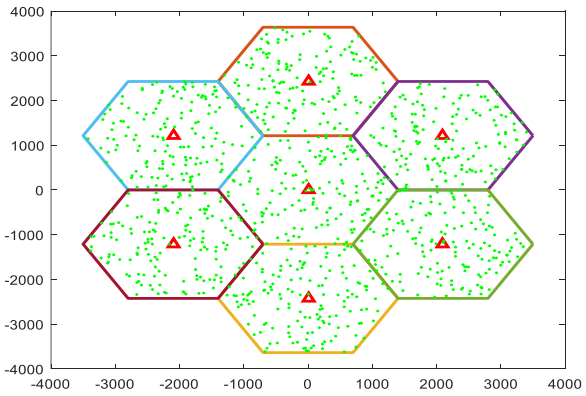

Fig. 1: The multi-cell multi-user mmWave MIMO model.

The channel gain between the k^{th} user of the j^{th} cell and the m^{th} base station antenna of the l^{th} cell is expressed as Eq. 1 (Mumtaz, Rodriguez, & Dai, 2017).

$$g_{jlkm} = \sqrt{\beta_{jlk}} h_{jlkm} \tag{1}$$

where β_{jlk} are large-scale fading coefficients which comprise path loss and shadow fading, which are invariant for the same BS, different antennas, and can be expressed as Eq. 2 (Mumtaz, Rodriguez, & Dai, 2017).

$$\beta_{jlk} = \frac{z_{jlk}}{\left(r_{jlk}/R\right)^a} \tag{2}$$

Where a is the path loss index, r_{jlk} is the range between the k^{th} user in the j^{th} cell and the l^{th} BS, z_{jlk} is the shadow fading and has a lognormal distribution, R is the radius of the cell, h_{jlkm} is the small-scale coefficient. The small-scale fading coefficients can be assumed to be independent and identically distributed. Due to reciprocity in communication networks, the uplink and downlink and block fading response, $h_{jlkm}$is the same for the length of coherence intervals, which range from 4 to 30 for OFDM symbols. The additive white Gaussian noise for all the mobile terminals are independently and identically distributed $(\mathcal{CN}(0,1)$ random variables. The channel matrix for the users in the j^{th} cell to the BS in the l^{th} cell can then be expressed as Eq. 3 (Gao, Hu, Dai, & Wang, 2016).

$$g_{jl} = D_{jl} H_{jl} \in \mathbb{C}^{K \times M} \tag{3}$$

Where $H_{jl} \in \mathbb{C}^{K \times M}$ are small-scale fading coefficients, i.e $[H_{jl}]_{km} = h_{jlkm}$; $D_{jl} \in \mathbb{C}^{K \times K}$is the diagonal matrix given as $[D_{jl}]_{k,k} = \sqrt{\beta_{jlk}}$. All the users in every cell transmit the pilot sequences of length τ symbols and it is given by Eq. 4 (Gao, Hu, Dai, & Wang, 2016).

$$\tau = N_c N_s \tag{4}$$

where N_c is the total symbols used for the pilots originating from the UEs to the BS, N_s is the number of consecutive subcarriers whose channel responses are constant during the frequency smooth interval (Marzetta, 2010). The BS has one uniform rectangular array (URA) with $N_T$antennas ($N_T = M$) and each UE N_R. The received signal of the kth UE in the jth cell $y_{j,k} \in \mathbb{C}^{M \times 1}$ is given as Eq. 5 (Marzetta, 2010).

$$y_{j,k} = \sum_{l=1}^{L} H_{jlk} x_l + n_{jk} \tag{5}$$

Where $H_{jlk} \in \mathbb{C}^{N_T \times N_R}$ is the channel gain matrix from the UEs in the j^{th} cell to the lth BS, $x_l \in \mathbb{C}^{N_T \times 1}$ is the transmitted signal input from the lth BS, $n_{jk} \in \mathbb{C}^{N_T \times 1}$ is the signal noise power received by the kth UE in the j^{th} cell which consists of the independently and identically distributed complex random variables with zero mean and variance σ^2. The mmWave MIMO network has a channel from the kth UE in the j^{th} cell to the lth BS, $H_{jlk} \in \mathbb{C}^{N_T \times N_R}$ is given as Eq. 6 (Mumtaz, Rodriguez, & Dai, 2017).

$$H_{jlk} = \sum_{n_p=1}^{N_P} \beta_{jl,pk} A_M\left(\theta_{jl,pk}^U, \emptyset_{jl,pk}^U\right) A_B^H\left(\theta_{jl,pk}^B, \emptyset_{jl,pk}^B\right) \tag{6}$$

where N_P is the number of paths, $\beta_{jl,pk}$is the complex path gain on the pth path from the kth UE in the j^{th} cell to the lth BS, $\theta^B_{jl,pk}, \emptyset^B_{jl,pk}$are the corresponding azimuth direction of departure and elevation direction of departure at the lth BS, respectively. $\theta^U_{jl,pk}, \emptyset^U_{jl,pk}$ are the corresponding azimuth direction of arrival and elevation direction of arrival at the kth UE in the j^{th} cell.

In real network implementation, the condition of perfect CSI availability to the BS is never met, and as such, it is usually estimated by the BS. Usually, the pilots in the uplink are used to estimate this channel. Since the coherence interval in a wireless fading channel and the orthogonal pilot sequences length are limited, the reuse of pilot sequences from the neighboring cells results in contamination of the CSI for a particular cell by the reuse of the same pilot in the neighboring cells (Figueiredo, Cardoso, Moerman, & Fraidenraich, 2017). This usually happens if the length of the pilots τ is not properly selected. Therefore, to reduce pilot contamination, the following scenario explains how the pilot length should be selected to minimize pilot contamination in a mmWave Multi-cell Massive MIMO network. Since the pilot sequence of the kth user can be given as in Eq. 7 (Figueiredo, Cardoso, Moerman, & Fraidenraich, 2017), where τ is the length of the pilots.

$$S_k = [s_k(0), \dots, s_k(\tau - 1)] \tag{7}$$

Then, by assuming $\tau < 2K$ since the number of pilot symbols is limited by coherence interval, but the valid pilots for the K users must satisfy the condition, $\tau \geq K$. For $\tau > KL$, the pilot contamination among the *L* cells for all the *K* users vanishes since the pilots are orthogonal, and they satisfy the condition $S_k = \tau I_k$. Therefore, the pilot length should fall in the range $K \leq \tau < 2K$. The pilot sequences for all the *K* users form a matrix **S** of dimensions $\tau \times K$. (Figueiredo, Cardoso, Moerman, & Fraidenraich, 2017; Zhu, Dai, & Wang, 2015)

The Zadoff Chu sequences are known to provide perfect autocorrelation and minimal cross-correlation properties. Thus, the pilots can have different cyclic shifts in each cell so that they can have orthogonality, and therefore the pilots are multiplied by phase shifts and reused amongst all other cells (Ke, Song, Ahmad, & Swamy, 2014). Then, the Chu sequence at the nth entry is given as Eq. 8 (Ke, Song, Ahmad, & Swamy, 2014).

$$\begin{aligned} \mathcal{A}_n &= [a_0, a_1, a_2, \dots, a_n], \quad \mathrm{n} = 1, 2, 3, \dots . \tau - 1 \\ &= \exp\left(i \frac{N\pi}{\tau}(n + \tau \, mod \, 2)\right) \end{aligned} \tag{8}$$

where N is an integer which is relatively prime to τ. The uplink pilot sequence received by the BS in the lth cell can be expressed in $M \times \tau$ matrix form as Eq. 9 (Al Imran, Hosain, & Shabab, 2022)

$$Y_l = \sqrt{\rho} \sum_{j=1}^{L} G_{jl} S_j^H + W_l \tag{9}$$

Where ρ is the signal-to-noise ratio of the transmitted signal, W_l is the $M \times \tau$ noise matrix. The noise is always considered even though the pilots are orthogonal. This is because there is a limited number of BS antennas, the presence of inter-user interference among adjacent channel vectors between users and cells, BS antennas are not orthogonal anymore and which causes pilot contamination. The pilot contamination should be minimized, and this is the main goal of this paper: to improve the sum rate of a multi-cell massive MIMO network. Taking into account all the interferences, the received sequence can be rewritten as Eq. 10 (Gao, Hu, Dai, & Wang, 2016).

$$Y_l = \sqrt{\rho} \sum_{j=1}^{L} G_{ll} S_j^H + \sqrt{\rho} \sum_{j=1, j \neq l}^{L} G_{jl} S_j^H + W_l \tag{10}$$

The first term is the desired pilot signals in the targeted cell, the second is the pilot signals from the adjacent cells (interfering pilot signals), and the third is the interfering noise signals. The pilot optimization can be introduced to improve the channel estimation performance (Nguyen, Nguyen, Nguyen, & Shin, 2018).

2.3. Multi-cell mmWave Massive MIMO Channel Estimation

2.3.1. Single Cell Channel Estimation

By employing the pilots, the CSI can be estimated for a single cell scenario. The BS estimates the status of the channels using LS or MMSE estimators. In LS, the kth column of S can be denoted as s_k. The channel estimation at BS l, $g_{llk}$with sufficient statistics provided can be given by Eq. 11 (Figueiredo, Cardoso, Moerman, & Fraidenraich, 2017).

$$Z_{lk} = \frac{1}{\sqrt{\rho\tau}} Y_l S_k^H = \sum_{l=1}^{L} g_{llk} + \mathcal{CN}(0, \frac{1}{\tau\rho} I_M \tag{11}$$

Then $Z_{lk} \sim \mathcal{CN}(0, \xi_{lk} I_M)$ where $\xi_{lk} = \sum_{l=1}^{L} \beta_{llk} + \frac{1}{\tau\rho}$. From this, the LS estimation is given by $\hat{g}^{LS}_{llk} = Z_{lk}$.The Minimum Squared Error (MSE) for each antenna given by the LS estimator is expressed as Eq. 12 (Figueiredo, Cardoso, Moerman, & Fraidenraich, 2017).

$$\eta^{LS}_{llk} = \frac{1}{M} E\left\{\left\|\hat{g}^{LS}_{llk} - g_{llk}\right\|^2\right\} = \xi_{lk} - \beta_{llk} \tag{12}$$

The normalized MSE for the LS can be given as Eq. 13 (Figueiredo, Cardoso, Moerman, & Fraidenraich, 2017).

$$NMSE_{LS} = \frac{E\left\{tr\left\{\left(\hat{G}_{jl} - G_{jl}\right)^H \left(G_{jl} - G_{jl}\right)\right\}\right\}}{E\left\{tr\left\{\hat{G}^H_{jl} G_{jl}\right\}\right\}} \tag{13}$$

The LS estimation is simple and doesn't require prior knowledge of the large-scale fading coefficients. For MMSE channel estimation, the prior knowledge of the statistical distribution properties is needed for the Bayesian MMSE channel estimator. The MMSE estimation is widely used in massive MIMO networks, and its channel estimation can be written as Eq. 14 (Figueiredo, Cardoso, Moerman, & Fraidenraich, 2017).

$$\hat{G}^{MMSE} = (S^H S + \sigma^2 I)^{-1} S^H Y_l \tag{14}$$

The ideal MMSE channel estimator can be defined as Eq. 15 (Figueiredo, Cardoso, Moerman, & Fraidenraich, 2017).

$$\hat{g}_{llk}^{MMSE} = \frac{\beta_{llk}}{\xi_{llk}} Z_{lk} \quad (15)$$

Each column of this follows $\mathcal{CN}(0, \frac{\beta_{llk}^2}{\xi_{lk}} I_M)$distribution. The MSE for each antenna is defined as Eq. 16 (Figueiredo, Cardoso, Moerman, & Fraidenraich, 2017);

$$\hat{n}_{lk}^{MMSE} = \frac{1}{M} E\left\{\left\|\hat{g}_{llk}^{MMSE} - g_{llk}\right\|^2\right\} = \beta_{llk}\left(1 - \frac{\beta_{llk}}{\xi_{llk}}\right) \quad (16)$$

The MSE of the MMSE channel estimator can be reduced when ρ increases and β_{llk}decreases.

2.3.2. Multi-cell mmWave Massive MIMO Channel Estimation

The matching filter-based channel estimation can be applied to the signal and the channel estimates as Eq. 17 (Ke, Song, Ahmad, & Swamy, 2014).

$$\hat{G}^{MF} = \left(diag(S^H S)\right)^{-1} S^H Y_l \quad (17)$$

The data-aided MMSE channel estimation technique uses the pilots and UE data for channel estimation. The LS estimate for the X_l uplink data matrix is given as Eq. 18 (Ke, Song, Ahmad, & Swamy, 2014).

$$\hat{G}_{jl} = \frac{1}{\sqrt{\rho\tau}} Y_l X_l^H (X_l X_l^H)^{-1} \quad (18)$$

Due to the mutual independent transmission of data symbols by the users, it can be observed that with perfect uplink data, the NMSE decreases as the data length goes to infinity. This implies that the pilot contamination vanishes for very large data length.

2.3.3. Channel Model of the mmWave Massive MIMO System

MmWave channels are divided into two major categories: physical models and analytical models. The foundation of physical models is the electromagnetic characteristics between the signal reception and transmission arrays. This type of model can effectively reflect measurement parameters and demonstrate the spatial correlation and sparsity of MIMO systems, and is also known as a parameterized model. It is commonly used in channel estimation and precoding design. Due to the limited number of scattering paths in mmWave propagation, most research work adopts geometric channel models to describe them. The current study also adopts the widely used Saleh-Valenzuela channel model.

Using the spherical wave model in a line-of-sight propagation scenario, we can define the propagation model of a mmWave channel. The channel vector for the k^{th} user in the l^{th} cell with an M-antenna array at the j^{th} cell is expressed as Eq. 19 (Mumtaz, Rodriguez, & Dai, 2017);

$$g_{jl,k} = \left(\frac{e^{\frac{2\pi}{\lambda} r_{jl,k_1}}}{r_{jl,k_1}}, \ldots, \frac{e^{\frac{2\pi}{\lambda} r_{jl,k_M}}}{r_{jl,k_M}}\right) \quad (19)$$

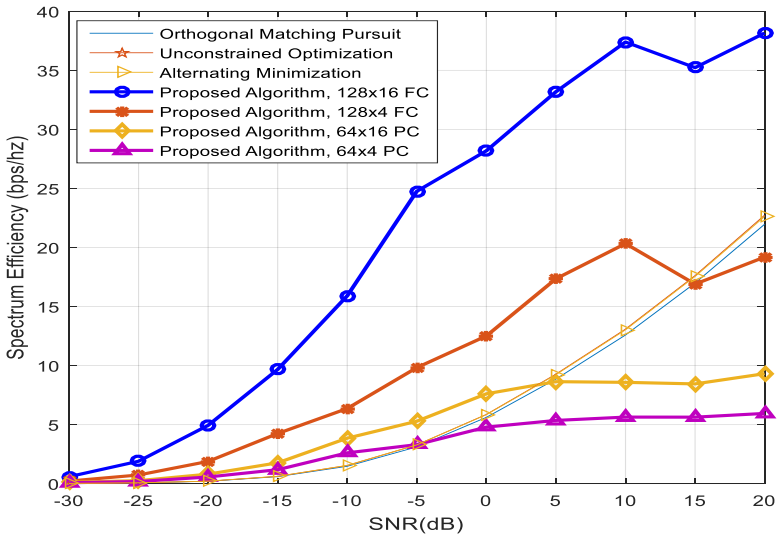

Fig. 2: Spectrum efficiency for full and partial connections.

Where r_{jl,k_M} is the distance from the k^{th} user in the l^{th} cell to the m-antenna in the j^{th} cell, λ is the wavelength of the carrier wave. The free space path loss model in mmWave can be given as in Eq. 20 (Mumtaz, Rodriguez, & Dai, 2017).

$$P_L = \left(\frac{4\pi d f_c}{c}\right)^2 \quad (20)$$

Where *f* is the carrier frequency in GHz, *d* is the distance from the transmitter in meters, and c is the velocity of light in a vacuum. The path loss can be expressed in dB as Eq. 21 (3GPP, 2020);

$$P_L(dB) = 32.45 + 20\log(f_c) + 20\log(d) \quad (21)$$

3. Results and Discussion

Fig. 2 shows the optimal spectrum efficiency for full connection and partial connection with N_T=128, N_R=4 and N_T=64, N_R=4 antenna arrays. The results show that a multi-antenna, multiuser system can greatly improve the capacity of the mmWave system, and it conforms with (Abose, Olwal, & Daniel, 2024). This is very useful as it enables users to achieve higher data rates for multimedia 5G services. In addition, the results show that the full connection (where every antenna is connected to an RF chain) scheme achieves a higher output than the partial connection (where a set of antennas shares an RF chain). Despite the full connection giving a higher performance, it has an effect of increasing power consumption, and as such, there needs to be a trade-off between higher capacity and power consumption for a full connection and a partial connection, depending on the type of application or service offer in 5G networks.

The proposed algorithm is then compared with a compressed sensing algorithm known as orthogonal matching pursuit (OMP), alternating minimization, and unconstrained algorithms. It was found that the proposed algorithm on a 128x16 MIMO network was, on average, 1.93 times better than the OMP algorithm, 3.41 times better than the unconstrained optimization algorithm, and 3 times better than the alternating optimization algorithm on a similar network scenario. For the 128x4 MIMO full connection, the proposed algorithm is 32.01% better than OMP, 72.57% better than unconstrained optimization, and 47.799% better than the alternating minimization algorithm. The 64x16 MIMO partial connection performs better than OMP, unconstrained optimization, and alternating minimization up to an SNR of 5dB. The 64x4 partial connection performs better than OMP, unconstrained optimization, and alternating minimization up to an SNR of 0dB. This is due to the limited beam forming gain in partially connected massive MIMO networks. In addition, the analog gain obtained from each antenna sub-array is also restricted. In fully connected networks, there is a greater degree of freedom in optimizing analog beam formers in all the antennas, which in turn improves the network performance.

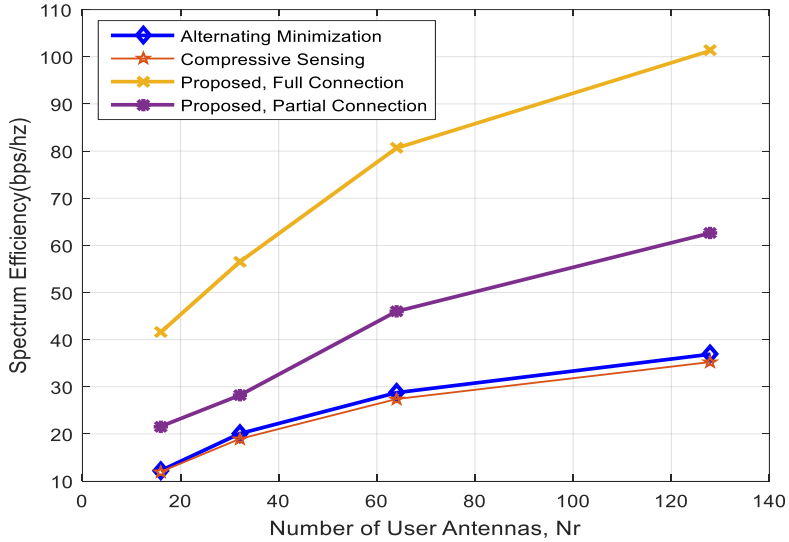

Fig. 3: Spectrum efficiency versus number of user antennas for N_T=128, N_R=128, SNR=10, L=7.

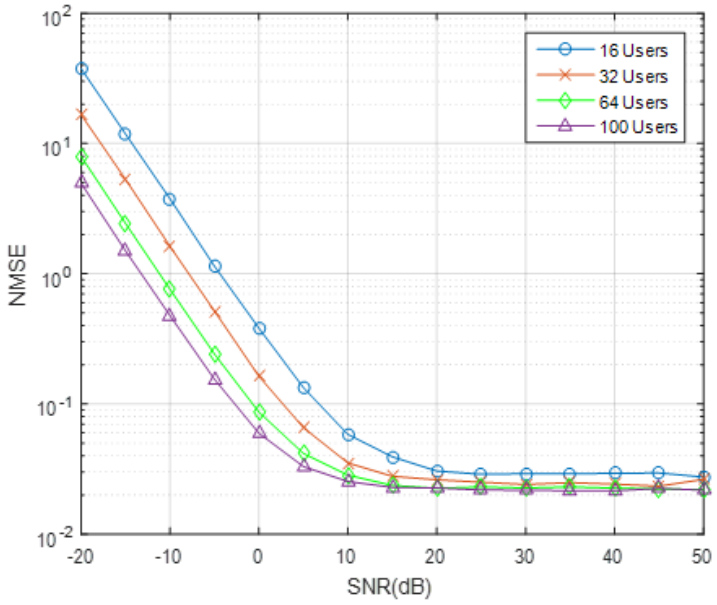

Fig. 4: Normalized MSE for different numbers of users

Fig. 3 shows a multi-cell MIMO scenario when SNR is held constant, and the number of receiver antennas varies from 8 to 128. It shows a greater improvement of about 2.5 times compared to a scenario when the SNR varies, and the number of receiver antennas is kept constant at 4. This shows how the use of multiple antennas in the transmitter and receiver for multi-user massive MIMO can greatly improve the sum rate of the network. For full connection, the proposed algorithm was found to be 1.94 times better than the alternating minimization algorithm and 2.067 times better than the compressive sensing algorithm. In partial connection, it was found to be 61.66% better than the alternating minimization algorithm and 68.62% better than the compressive sensing algorithm.

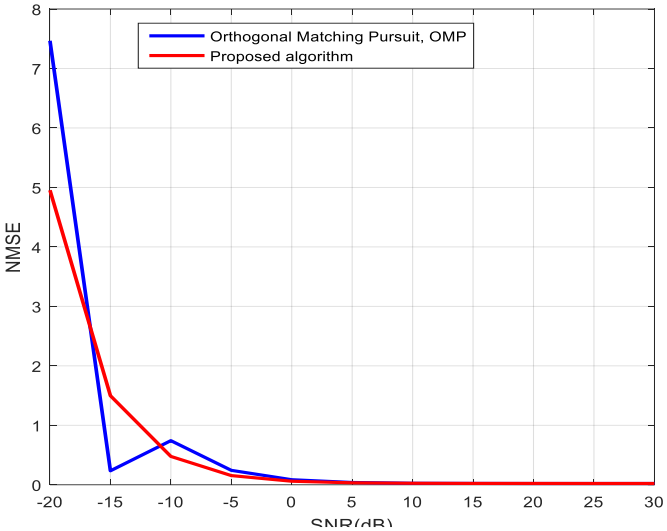

Fig. 5: NMSE for varying transmitter antennas

Fig. 4 shows the normalized minimum square error for different numbers of users for N_T=128, N_R=128. In this scenario, clustering of users is allowed for those close to each other. It is shown that with a dense number of users, the performance is better compared to a low number of users. This is due to the ease of forming clusters when the number of users increases, and they can now be handled as a group instead of individual users. It has also been shown that the SNR of such a network should be set as a minimum of 10dB since the NMSE remains almost constant beyond this point. Therefore, the SNR the network should be operating should be chosen depending on the power allocation scheme deployed for such a network. When comparing the proposed algorithm with the Orthogonal Matching Pursuit (OMP) algorithm for 100 users, it was found that the NMSE error reduces by an average of 35.601% as shown in Fig. 5.

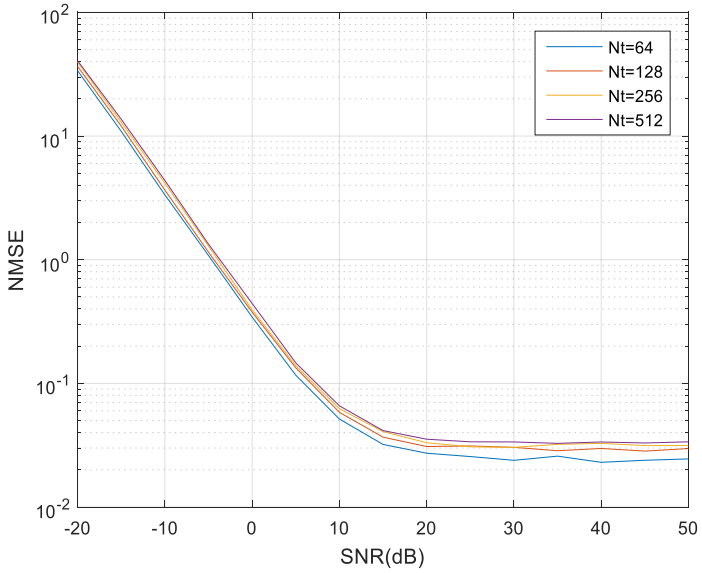

Fig. 6: NMSE for varying transmitter antennas

Fig. 6 shows the NMSE for different numbers of antennas at the transmitter. It has been shown that increasing the number of antennas at the transmitter increases the error attained. This is due to the increase in the number of RF chains when the number of antennas goes up. Fig. 7 shows the validation of the SVD-based algorithm by comparing its performance with a compressive sensing algorithm presented in (Gao, Mei, &

Qiao, 2022; Oyerinde, Flizikowski, & Marciniak, 2022) in full connection mode for N_T=128, N_R=4. It was shown that the proposed algorithm improved the spectrum efficiency by an average of factor of 1.6381.

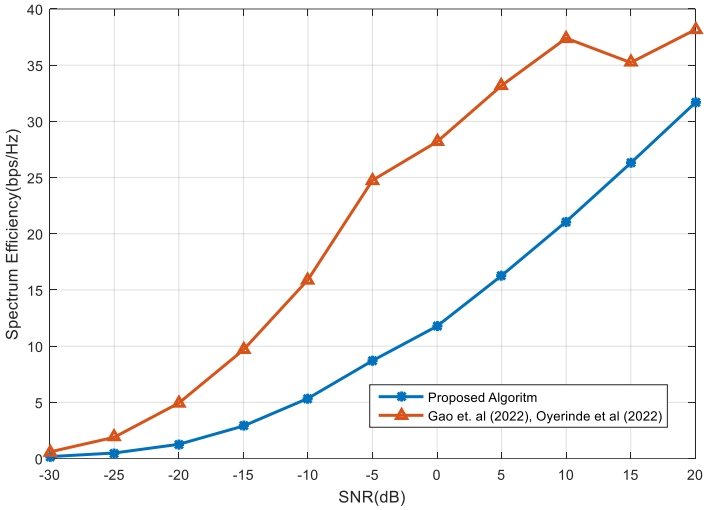

Fig. 7: Comparison of spectrum efficiency for full connection (N_T=128, N_R=4)

4. Conclusion

The study considered the problem of hybrid precoding and combiner design in a multi-cell, multiuser mmWave massive MIMO network for 5G applications. The hybrid precoding scheme was modelled and a mathematical problem formulated to maximize spectrum efficiency and minimize the normalized minimum square error by varying the number of users, number of antennas at the transmitter and receiver, and the signal to noise ratio. The solution was provided by the proposed single value decomposition-based algorithm, which synthesizes the MIMO system into a set of multiple SISO channels. Then, channel estimation was applied for the downlink transmission in the developed model. The results show that the network performance can be improved in a mmWave massive MIMO network in terms of spectrum efficiency by careful selection of the number of antennas in the transmitter and receiver, the number of RF chains, and transmission paths or rays. In addition, allowing clustering of users in a multi-cell scenario can greatly improve the spectrum efficiency and support a greater number of users with minimal interference between the users and between cells. The main challenge in this study was the need for more computational resources due to the rise in user density and the large-scale deployment of MIMO antennas. This can be addressed by incorporating optimal machine learning tools in the management of interference for the developed multi-cell MIMO network.

References

3GPP. (2020). Study on Channel Model for Frequencies from 0.5 to 100GHz (Release 16). Retrieved July 22, 2020, from https://portal.3gpp.org/#/55936-specifications

Abose, T. A., Olwal, T. O., & Daniel, A. D. (2024). Performance Comparison of Hybrid Switch, Phase Shifter and Lens Network over Hybrid Beamforming in Millimeter Wave Massive MIMO. *Iranian Journal of Eletrical and Electronic Engineering*, 20(3).

Al Imran, M. I., Hosain, M. F., & Shabab, R. (2022). Hybrid Precoder Design Using Alternating Minimization Algorithm in MultiCell Multi-User Millimeter-Wave Communications for Massive MIMO. *International Conference on Electronic Circuits and Signalling Technologies*. Coimbatore, India.

Ally, J. (2023). Evaluation of Linear Precoding Schemes for Cooperative Multi-cell MU MIMO in Future Mobile Communication Systems. *Journal of Computer and Communications*, 11(6), 28-42.

Chen, C. H., Tsai, C. R., Liu, Y. H., Hung, W. L., & Wu, A. Y. (2016). Compressive Sensing Assisted Lo-Complexity Beamspace Hybrid Precoding for Millimeter-wave MIMO Systems. *IEEE Transactions on Signal Processing*, 65(6), 1412-1424.

Figueiredo, F. A., Cardoso, F. A., Moerman, I., & Fraidenraich, G. (2017). Channel Estimation for Massive MIMO TDD Systems Assuming Pilot Contamination and Frequency Selective Fading. *IEEE Access*, 5, 17733-17744.

Gao, Z., Hu, C., Dai, L., & Wang, Z. (2016). Channel Estimation for Millimeter-Wave Massive MIMO with hybrid Precoding over Frequency-Selective Fading Channels. *IEEE Communications Letters*, 20(6), 1259-1262.

Gao, Z., Mei, Y., & Qiao, L. (2022). Compressive Sensing Sparse Channel Estimation in Broadband Millimeter-Wave Massive MIMO Systems. Sparse Signal Processing for Massive MIMO Systems. 17, pp. 2946-2960. Singapore: Springer Nature.

Hao, Z., Luo, Z., Li, X., & Fan, J. (2024). Tensor-based Channel Estimation for Millimeter Wave MIMO by Exploiting Sparsity in Delay-Angular Domain. *IEEE Transactions on Communications*, 23(12), 9259-19274.

Heath, R. W., Gonzalez-Prelcic, N., Ranguan, S., Roh, W., & Sayeed, A. M. (2016). An Overview of Signal Processing Techniques for Millimeter Wave MIMO Systems. *IEEE Journal of Selected Topics in Signal Processing*, 10(3), 436-453.

Hong, J., Sun, J., He, Y., Zhang, W., & Wang, C. X. (2024).

A Tensor-Based Millimeter Wave Wideband Massive MIMO Channel Estimation Technique Using Uniform Planar Arrays. *IEEE Wirelesss Communications Letters*, 13(5), 1458-1462.

Hu, A. (2018). Beam Grouping Based User Sceduling in Multicell Millimeter-Wave MIMO Systems. IEEE Access, 6, 55004-55012.

Ke, L., Song, X., Ahmad, O. M., & Swamy, M. N. (2014). An improved multicell MMSE channel estimation in a massive MIMO system. *International Journal of Antennas and Propagation*, 2014(1), 387436.

Kim, H., Gil, G. T., & Lee, Y. H. (2019). Two-Step Approach for Wideband Millimeter Wave Systems with Hybrid Architecture. *IEEE transsctions on Communications*, 67(7), 5139-5152.

Kodimyala, S., & Tadisetty, S. (2022). Uplink millimeter-wave multi-cell multi-user massive multi-input multi-output systems. *Indonesian Journal of Electrical Engineering and Computer Science*, 26(1), 261-268.

Kondapalli, P., Kumari, K. A., Kiranmai, B., Iavanya, ,. V., Venkata, Y., Lakshami, B., & Tammineni, V. (2024). Optimized Hybrid Precoding for Energy and Spectrum Efficiency in mmWave Massive MIMO System. *Journal of Electrical Systems*, 20(11s), 1683-1691.

Li, K., Song, X., Ahmad, M. O., & Swamy, M. N. (2014). An Improved Multi-cell MMSE Channel Estimation in a Massive MIMO System. *International Journal of Antennas and Propagation*, 2014(1), 387436.

Liu, Y. B., & Wang, Y. (2024). An Efficient mmWave MIMO Transmission with Hybrid Precoding. *KSII Transactions on Internet and Information Systems*, 18(7), 2010-2026.

Lu, z., Guo, Y., Yang, W., Liu, Y., Luan, Q., & Mei, Y. (2020). Hybrid Beamforming in Multiuser mmWave Massive MIMO System. *2nd International Conference on Electronics and Communication, Network and Computer Technology*. Chngdu, China.

Majidzadeh, M., Kaleya, J., Tervo, N., Pennanen, H., Tolli, A., & Latva-aho, M. (2024). Hybrid Beamforming for mmWave Massive MIMO Systems with partially Connected RF Architecture. *Wireless Personal Communications*, 136(4), 1947-1979.

Marzetta, T. L. (2010). Noncooperative cellular wireless with unlimited numbers of base station antennas. *IEEE Transactions on Wireless Communications*, 9(11), 3590-3600.

Moradi, A., & Farsani, N. J. (2024). A Dynamic Hybrid Precoding Structure for mmWave Massive MIMO Systems. *International Journal of Information and Communication Technology*, 16(1), 1-10.

Mumtaz, S., Rodriguez, J., & Dai, L. (2017). mmWave Massive MIMO: A Paradigm for 5G. London: Academic Press.

Nguyen, H. V., Nguyen, V., Nguyen, H. M., & Shin, O. S. (2018). Uplink training with Pilot Optimization for Multicell Massive MIMO Systems. *IET Communications*, 1-9.

Oyerinde, O. O., Flizikowski, A., & Marciniak, T. (2022). Compressive Sensing-based Channel Estimation Schemes for Wideband Millimeter Wave Wireless Communication. *Computers and Electrical Engineering*, 104, 108452.

Raj, S., Gilbert, M., & Bala, G. J. (2021). Millimeter-wave Massive MIMO Channel Estimation based on Majorization-minimization Approach. *Physical Communication*, 47.

Riadi, A., Boulouird, M., & Hassani, M. M. (2019). Performance of Massive -MIMO OFDM System with M-QAM Modulation based on LS Channel Estimation. *International Conference on Advanced Ssystems and Emergent Technologies*, (pp. 74-78). Hammamet.

Riviello, D. G., Di Stacio, F., & Tuninato, R. (2022). Performance Analysis of Multi-user MIMO Schemes under Realistic 3GPP 3-D Channel Model for 5G mmWave cellular networks. *Electronics*, 11(3), 330.

Rodriguez-Fernandez, J., Gonzalez-Prelcic, N., Venugopal, K., & Heath, R. W. (2018). Frequency Domain Compressive Channel Estimation for Frequency Selective Hybrid mmWave MIMO Systems. *IEEE Transactions of Wireless Communication*, 17(5), 2946-2960.

Samir, Y. N., Nafea, H. B., & Zaki, F. W. (2023). Performance Evaluation of Spectral Efficiency Hybrid Precoding and Combinging Algorithm for Millimeter Wave MIMO. *Wireless Personal Communications*, 133(3), 1769-1784.

Sha, Z., Wang, Z., Chen, S., & Hanzo, L. (2020). Graph Theory Based Beam Scheduling for Inter-Cell Interference Avoidaance in mmWavr Cellular Networks. *IEEE Transacions on Vehicular Technology*, 69(4), 3929-3942.

V., M. P., & Ramana, T. V. (2025). Adaptive Precoding for Reliable Multi-user mmwave MIMO Systems. *Progress in Electromagnetics Research C*, 152, 171-176.

Vadgaye, R. M., & Manjula, S. (2024). Advanced Spatial Adaptive Channel Estimation for Efficient mmWave Communication. *Bulletin of Electrical Engineering and Informatics*, 13(6), 4069-4078.

Vlachos, E., Alexandropoulos, G. C., & Thompson, J. (2019). Wideband MIMO Channel Estimation for Hybrid Beamforming Millimeter Wave Systems. *IEEE Journal of Selected Topics in Signal Processing*, 13(5), 1136-1150.

Wang, B., Jian, M., Gao, F., Li, G. Y., & Lin, H. (2019). Beam Squint and Channel Estimation for Wideband mmWave Massive MIMO-OFDM Systems. *IEEE Transactions on SIgnal Processing*, 67(23), 5893-5908.

Xu, L., Cheng, L., Wong, N., Wu, Y. C., & Poor, H. V. (2024). Overcoming Beam Squint in mmwave MIMO Channel Estimation; A Bayesian Multi-Band Sparsity Approach. *IEEE Transactions on Signal Processing*, 72, 1219-1234.

Zhu, X., Dai, L., & Wang, Z. (2015). Graph Coloring based Pilot Allocation to Mitigate Pilot Contamination For MultiCell Massive MIMO Systems. *IEEE Communication Letters*, 19(10), 1842-184.